Original Article

Development of bone seeker–functionalised microspheres as a targeted local antibiotic delivery system for bone infections

Stijn G. Rotman [a,b], Keith Thompson [a], Dirk W. Grijpma [b], Robert G. Richards [a], Thomas F. Moriarty [a], David Eglin [a], Olivier Guillaume [a,*,☆]

[a] Musculoskeletal Regeneration Program, AO Research Institute Davos, Davos, Switzerland
[b] Department of Biomaterials Science and Technology, Faculty of Science and Technology, Technical Medical Centre, University of Twente, Enschede, the Netherlands

ABSTRACT

Objective: Bone infections are challenging to treat because of limited capability of systemic antibiotics to accumulate at the bone site. To enhance therapeutic action, systemic treatments are commonly combined with local antibiotic-loaded materials. Nevertheless, available drug carriers have undesirable properties, including inappropriate antibiotic release profiles and nonbiodegradability. To alleviate such limitations, we aim to develop a drug delivery system (DDS) for local administration that can interact strongly with bone mineral, releasing antibiotics at the infected bone site.

Methods: Biodegradable polyesters (poly (ε-caprolactone) or poly (D,L-lactic acid)) were selected to fabricate antibiotic-loaded microspheres by oil in water emulsion. Antibiotic release and antimicrobial effects on *Staphylococcus aureus* were assessed by zone of inhibition measurements. Microsphere bone affinity was increased by functionalising the bisphosphonate drug alendronate to the microsphere surface using carbodiimide chemistry. Effect of bone targeting microspheres on bone homeostasis was tested by looking at the resorption potential of osteoclasts exposed to the developed microspheres.

Results: In vitro, the antibiotic release profile from the microspheres was shown to be dependent on the polymer used and the microsphere preparation method. Mineral binding assays revealed that microsphere surface modification with alendronate significantly enhanced interaction with bone-like materials. Additionally, alendronate functionalised microspheres did not differentially affect osteoclast mineral resorption *in vitro,* compared with nonfunctionalised microspheres.

Conclusion: We report the development and characterisation of a DDS which can release antibiotics in a sustained manner. Surface-grafted alendronate groups enhanced bone affinity of the microsphere construct, resulting in a bone targeting DDS.

The Translational Potential of this Article: The DDS presented can be loaded with hydrophobic antibiotics, representing a potential, versatile and biodegradable candidate to locally treat bone infection.

Introduction

Infection of bone, also known as osteomyelitis (OM), is challenging to treat by systemic antibiotic administration because of impaired vascularity of infected bone tissue [1], limited capacity of bone tissue to retain drugs for long periods of time and a poor ability of many common antibiotics to effectively penetrate infected bone [2]. All of these factors can result in an insufficient local antibiotic concentration that is then unable to clear the infection successfully [3]. Consequently, the current consensus for OM treatment is an initial debridement of infected tissues followed by the synergetic use of systemically administered antibiotics and local drug delivery systems (DDSs) that can locally release antibiotics over an extended period of time. However, combination of therapy is not always successful in treating chronic OM, as reinfection rates are still relatively high and can reach approximately 30% for patients with complicated open bone fractures [4]. One of the main reasons for

reinfection originates in the inability of the antibiotic to reach a sufficiently high concentration within infected bone tissue, where viable bacteria may remain.

Gentamicin sulfate (GEN) is a broad-spectrum antibiotic used to treat blood, skin, lung, joint and bone infections. In addition, owing to GEN's heat stability, it is one of the most frequently used antibiotics for exothermically setting poly (methyl methacrylate) (PMMA) bone cements [5]. GEN-loaded PMMA cements are frequently implanted as a local DDS, either as a prophylactic approach or as a treatment for bone infections since the 1970s. However, a particular disadvantage of PMMA is its nondegradability and incomplete drug release [6], necessitating a further surgical procedure to remove PMMA cements. Such limitations motivate the search for an alternative degradable and more versatile material to be used for local antibiotic delivery strategies.

Loading GEN in degradable DDS has also been proposed, but it often results in a fast elution because of its high solubility in aqueous solutions and low affinity to hydrophobic matrices [7]. Being a salt, GEN can undergo hydrophobic ion pairing to impose hydrophobic properties to the drug. By substituting the sulfate ion of GEN with other anions such as crobefate [8] or pamoate ions (gentamicin embonate), hydrophobicity and matrix affinity increases. We have previously synthesised a hydrophobic GEN analogue, gentamicin-dioctyl sulfosuccinate (GEN-AOT) following established protocols [9,10]. Water solubility of GEN-AOT (0.43 mg/mL) is dramatically reduced compared with GEN (100 mg/mL), but it maintains antimicrobial activity against *Staphylococcus aureus* and *Staphylococcus epidermidis*, comparable to GEN [9].

Frequently applied materials for DDS development are biodegradable polyesters such as poly (D,L-lactic acid) (PDLLA) [11], poly (lactic-co-glycolic acid) (PLGA) [12] and poly (ε-caprolactone) (PCL) [13]. The respective monomers and their isomeric composition dictate their degradation behaviour. Poly (lactic acid) with only L-isomers is more crystalline compared with poly (lactic acid) with both L-isomer and D-isomer (PDLLA), making PDLLA more susceptible to hydrolysis. PCL does not have optical isomers and can be considered a hydrophobic semicrystalline polymer. This results in slower *in vivo* degradation compared with the other members of the polyester family such as PLGA [14]. This information highlights the importance of material choice in designing a DDS.

The majority of DDS previously reported do not exhibit intrinsic affinity to bone, which limits their clinical potential for drug delivery to bone. However, there are many molecules available that exhibit affinity to bone, which can be used to generate bone targeting DDS. The use of so called 'bone seeking' or 'bone binding' agents combined with DDS have brought promising preclinical and clinical solutions to treat bone-related disorders and were recently reviewed [15]. The inorganic matrix of bone, consisting of hydroxyapatite (HAP) crystals, is often targeted by these bone binding molecules. As an example, bisphosphonates (BPs) are known for their rapid and strong binding to calcium ions in HAP via chelation, facilitated by their two phosphonate groups [16]. The BP alendronate (ALN) is frequently incorporated into DDSs [17–19], as its side chain contains a reactive primary amine that is available for conjugation chemistry.

In this work, we synthesised and characterised a degradable microsphere DDS, loaded with GEN-AOT antibiotic *in vitro*. We assessed binding capabilities of ALN functionalised PCL microspheres to bone and *in vitro* efficacy of the antibiotic released from the DDS. Drug delivery to bone has been undertaken in the field of osteosarcoma (e.g. by delivery of doxorubicin [20]) and osteoporosis (e.g. by delivery of simvastatin [21]), but often these delivery systems do not show inherent affinity to bone. To the best of our knowledge, such DDS for antibiotics have not been reported in the field of bone infection. Compared with laborious (amphiphilic) co-polymer strategies reported in the literature [22], the presented DDS can be fabricated from common PCL with minimal post-treatment procedures to enhance its affinity to HAP. Such active DDS represents a promising, versatile and up-scalable candidate to improve the local treatment of bone infection.

Materials and methods

Materials

PCL (M_w = 80.000 g mol^{-1}, polydispersity index < 2), boric acid, pyrene, o-phthaldialdehyde, methanol, hydrochloric acid, N-hydroxysuccinimide (NHS), dioctyl sodium sulfosuccinate sodium salt (AOT), silver nitrate, sodium thiosulfate, GEN salt, phosphate buffered saline (PBS), tartrate-resistant acid phosphatase (TRAP) staining kit and alendronate sodium were purchased from Sigma Aldrich (Steinheim, Germany). PDLLA (M_w = 215.000 g mol^{-1}, 80% L, 20% D:L) was bought from Corbion Purac (Gorinchem, the Netherlands). Poly (vinyl alcohol) (PVA, M_w = 31.000 g mol^{-1}), sodium hydroxide (NaOH), dichloromethane (CH$_2$Cl$_2$), dimethyl sulfoxide (DMSO) and 2-propanol was bought from Carl Roth (Karlsruhe, Germany). 1-Ethyl-3-(3-dimethylaminopropyl)carbodiimide (EDC) was purchased from Fluka (Buchs, Switzerland) (5-((2-Aminoethyl)amino)naphthalene-1-sulfonic acid) (EDANS) was bought from Anaspec (Seraing, Belgium). Tryptone soy agar (TSA) was purchased from Oxoid AG (Basel, Switzerland). Alpha minimum essential media, fetal bovine serum and penicillin/streptomycin were bought from Gibco (Zug, Switzerland). Receptor activator of nuclear factor kappa-B ligand and macrophage-colony stimulating factor (MCSF) growth factors were purchased from R&D Systems (Abingdon, UK). Osteoassay plates were acquired from Corning (Amsterdam, the Netherlands). Ultra-pure milliQ water (18.2 MΩ cm) was used during all experiments. Methacrylated-Poly (trimethylene carbonate) scaffolds containing 40 wt% dispersed nanohydroxyapatite were kindly provided from collaborators at the University of Twente (Enschede, the Netherlands) and were prepared as previously described [23].

GEN-AOT synthesis by hydrophobic ion pairing

GEN-AOT was synthesised as described by ter Boo et al. [9]. Briefly, equal volumes of 1.25% w/v AOT in CH$_2$Cl$_2$ and 0.40% w/v GEN in buffer (10 mM sodium acetate, KCl and CaCl$_2$ at pH = 5) were mixed by vigorous stirring for 3 h. The two phases separated for 30 min, and GEN-AOT was isolated from the dichloromethane by evaporation of the solvent. Fourier transform infrared spectroscopy characterisation was performed to validate the successful pairing of AOT with GEN (Figure S1). The water solubility of GEN-AOT was determined by complexation of saturated aqueous solutions with o-phthaldialdehyde reagent in a colorimetric assay, at a wavelength of 332 nm using a spectrophotometer (MultiskanGo, Thermo Scientific) [24].

Fabrication of PCL and PDLLA microspheres loaded with GEN-AOT or pyrene

PCL or PDLLA (500 mg) was dissolved in 5 mL CH$_2$Cl$_2$. As encapsulated compounds, 25% w/w GEN-AOT or 10% w/w pyrene (used as a probe for a fluorimetic assay) relative to the weight of the polymer was added to the polymers in solution. PVA solution (100 mL, 1% w/v) acted as the aqueous phase during the emulsion process. Emulsions were prepared by probe sonication (Bandelin Sonopuls GM70, 3 bursts of 10 s, 700 W) or by ultra-turrax homogenisation (Silverson LM5, 10 min at 10.000 rpm). Under moderate stirring, the organic solvent was evaporated over 4 h at room temperature, resulting in solidified microspheres. The microspheres were collected by centrifugation at 68.000*g* with an ultracentrifuge (Sorvall Discovery 90 SE) and were washed and resuspended twice with milliQ water to remove the excess of the PVA surfactant. The microspheres were then lyophilised and stored at 4°C until utilisation. To determine drug loading, GEN-AOT loaded microspheres were placed in 1 M NaOH to hydrolyse the microspheres, and GEN-AOT was subsequently quantified after complexation with o-phthaldialdehyde reagent as previously described [24]. The encapsulation efficiency (EE%) of the microspheres is calculated following equation (1):

$$EE\% = \left(GEN - AOT_{Encapsulated} \middle/ GEN - AOT_{Initial}\right) \cdot 100\% \tag{1}$$

With GEN-AOT$_{Encapsulated}$ as the amount of GEN-AOT spectrophotometrically quantified and GEN-AOT$_{Initial}$ as the amount of GEN-AOT added to the emulsion system. To ensure batch-to-batch reproducibility, another batch was fabricated under identical circumstances.

Release profile of GEN-AOT from PCL and PDLLA microspheres

10 mg of GEN-AOT loaded microspheres (n = 6) were incubated in 1 mL of PBS at 37°C under mild shaking (30 rpm). At each time point (2 h, 6 h, 1 day, 2 days, 3 days, 6 days, 12 days and 14 days), the samples were centrifuged at 16.000g for 10 min (Eppendorf centrifuge 5415D), and the supernatants were carefully removed. At each timepoint, the PBS was replaced with 1 mL of fresh PBS. Supernatants were assessed for their GEN-AOT content, as previously described.

Surface functionalisation with EDANS or ALN

The functionalisation of the polyester-based microspheres required initial surface hydrolysis to increase the fraction of carboxylic groups. The lyophilised microspheres were dispersed in 0.1 M NaOH solution (10 mg/mL), and the microspheres' surface were saponified (alkaline induced hydrolysis) for 30, 60 or 120 min. To terminate the saponification process, 2 mL of 1 M hydrochloric acid was added to facilitate the formation of carboxyl groups (-COOH) from the formed COO–Na$^+$ ionic chain ends. The microspheres were collected by centrifugation for 15 min at 68.000 g and washed in milliQ water. The saponified microspheres were then dispersed in 10 mL 2-(N-morpholino)ethanesulfonic acid-buffer (pH = 5.5) containing EDC (50 mg, 0.26 mmol) and NHS (50 mg, 0.43 mmol). The microspheres underwent carboxyl activation for 30, 60 or 120 min and were collected by centrifugation for 15 min at 68.000 g, followed by washing in milliQ water. To assess the ability of compounds with primary amine groups to be conjugated to the microspheres by EDC/NHS chemistry, the microspheres were dispersed in 2 mL of aqueous solution of fluorescent EDANS (250 µg/mL), and conjugation was allowed to proceed for 60 min under mild stirring at room temperature. The relative amount of surface grafted EDANS was measured using a fluorescence plate reader (*Viktor*[3], PerkinElmer) at 461 nm. For ALN conjugation, 30 min of saponification and 30 min of EDC/NHS activation were used based on satisfactory surface conjugation of EDANS.

To monitor the effect of NaOH exposure to the molecular weight of the PCL polymers, gel permeation chromatography (GPC) was performed. PCL microspheres and saponificated PCL microspheres (30 min) were dissolved in chloroform (1 mg/mL) and injected into the GPC system (Agilent 6850).

PCL-ALN affinity to bone-like material

Pyrene was chosen as an internalised fluorophore to assess the microparticle affinity to HAP. Pyrene encapsulation in PCL microspheres and surface functionalisation with ALN was performed as described earlier in this work. To perform the HAP binding assay, a bone-like methacrylated-poly (trimethylene carbonate) scaffold containing 40% w/w of dispersed nano-HAP powder, made by stereolithography, was used as a macroscopic binding substrate. The fabrication methods of these scaffold materials can be found in previous publications [23,25]. The fabricated nano-HAP scaffolds were incubated for 2 h in a 500 µg/mL PCL-ALN or PCL microsphere dispersion as control. After incubation, the scaffolds were thoroughly washed with distilled water to remove non-chelated microspheres from the surface. Fluorescence from the scaffolds incubated with pyrene-loaded PCL, and PCL-ALN microspheres was measured on a Viktor[3] plate reader (PerkinElmer) with $\lambda_{ex}/\lambda_{em} \sim 353$ nm/483 nm.

Inhibitory effect of ALN-functionalised microspheres on osteoclasts

Monocyte/macrophage-lineage osteoclast precursors were isolated from the bone marrow of female, balb/c mice, n = 2, according to guidelines of the cantonal authorities (Tierversuchskommission Graubünden) and were kindly donated by the Swiss Institute of Allergy and Asthma Research (TVB number: 27653; Cantonal number: GR 2016_02F). The osteoclast precursors were cultured in standard culture conditions (37°C, 5% CO_2) with αMEM supplemented with 10% v/v fetal bovine serum, 1% v/v penicillin/streptomycin and 50 ng/mL of recombinant murine MCSF. After 5–7 days, 10 ng/mL of recombinant murine receptor activator of nuclear factor kappa-B ligand was added to the culture medium to support the fusion of osteoclast precursors into osteoclasts. After 48 h, the osteoclasts were trypsinised and seeded on Osteoassay 96-well at a density of 10^4 cells/well. After allowing the cells to attach to the substrate for 4 h, 10 µM ALN solution in PBS or 1.7 mg of PCL and PCL-ALN microspheres were added to the respective wells. This quantity of PCL-ALN particles corresponded to 10 µM of surface grafted ALN, as established by spectrophotometrical analysis of EDANS grafting. After 72 h, the cells and microspheres were washed twice with PBS, and the content of the wells was fixed using 4% formaldehyde solution for 15 min at room temperature. The osteoclasts were stained with a TRAP staining kit prior to brightfield microscopy imaging. After assessing the osteoclast morphology, the cells were removed by using 10% v/v bleach, and the HAP substrate was stained with a Von Kossa silver nitrate stain to visualise HAP resorption and imaged using an inverse light microscopy (Zeiss Axiovert.A1). The area of stained mineral was quantified after binarisation of the image using AxioVision 4 software (Zeiss).

In vitro antimicrobial assessment

The minimal inhibitory concentration (MIC) and minimal bactericidal concentration (MBC) was determined by supplementing GEN-AOT–loaded PCL, GEN-AOT or GEN in the *S. aureus* CAMH culture broth. Antibiotic solutions and particle dispersions in CAMH broth were made by 1:1 dilution to achieve the range of 500 µg/mL to 0.49 µg/mL (GEN and GEN-AOT) or 5000 µg/mL to 5 µg/mL (PCL/GEN-AOT microspheres). GEN-AOT was initially dissolved in DMSO and was subsequently 1:9 diluted with CAMH broth to reach comparable concentrations with GEN. The final content of the wells of a 96-well plate was 100 µL *S. aureus* inoculum (10^5 CFU/mL) and 100 µL antibiotic solution or particle dispersion. The cultures were incubated for 24 h at 37°C and 5% CO_2, after which 100 µL per condition was plated on a TSA plate to quantify the CFU. All conditions were measured in triplicate.

Time dependent inhibitory properties of the GEN-AOT–loaded PCL microspheres were assessed with zone of inhibition (ZOI) experiments. *S. aureus* were cultured on TSA plates in standard culture conditions of 37°C and 5% CO_2. In the centre of the TSA plate, 10 mg of GEN-AOT–loaded microspheres were deposited on a sterile wafer (Sensi-disc, BD Biosciences) and wetted with 20 µL of PBS. The wafer was transferred daily to a freshly plated *S. aureus* culture and incubated for 24 h. The radius of the *S. aureus*-free zone around the antimicrobial sample was measured daily. A 50 mg/mL GEN-AOT solution in DMSO in a volume of 20 µL was used to mimic a single systemic drug administration. Two clinical reference DDS were assessed as positive controls for their ability to inhibit *S. aureus* growth: A collagen-fleece material loaded with Gentamicin sulfate (Garamycin®) was cut in the size of 1 cm^2 (containing approximately 1.3 mg of Gentamicin sulfate) and 110 ± 5 mg of PMMA bone cement (Copal®, containing approximately 1.3 mg of Gentamicin sulfate and 5.2 mg of Vancomycin).

Scanning electron microscopy imaging

Lyophilised microsphere samples before and after surface conjugation with ALN were dispersed in ethanol, and 40 µL of the microsphere dispersion was pipetted on scanning electron microscopy (SEM) pin stub

specimen mounts covered with a conductive adhesive layer. The ethanol was evaporated at room temperature. The samples were then sputter-coated with Au/Pd with a layer thickness of 10 nm and a deposit rate of 0.05 nm/s. SEM imaging was performed on a field emission scanning electron microscope (S-4700, Hitachi). The working distance of the SEM was maintained at approximately 8 mm, and an acceleration beam voltage of 1.5 keV was used. For microsphere size analysis, the diameter of a minimum of 100 PCL or PDLLA microspheres were measured to achieve a reliable and representable size average.

Statistical analysis

Statistical significance was assessed using GraphPad Prism software. One-way analysis of variance with Bonferroni posttest was applied on multivariable data that were tested for normality by Q–Q plot interpretation. When data with a single variable were analysed, Student unpaired t test with a Tukey posttest was used with a confidence interval of 95%.

Results

Nature of the matrix and fabrication method influence microsphere size and drug encapsulation

The size distribution, average microsphere diameter (Ø), the EE% of GEN-AOT and surface morphology of the four different microsphere formulations are shown in Figure 1. The two variables assessed were the nature of the polymeric matrix (PCL or PDLLA) and the method of emulsification (probe sonication [SON] or high-speed mechanical mixing by ultra-turrax [HSM]). Figure 1A shows that the use of PDLLA resulted in right-sided skewness in size distribution which in turn resulted in higher Ø values, in comparison to PCL microspheres. The method of emulsification also impacted on their diameter. The use of HSM resulted in a wider size distribution compared emulsions made by SON. EE% of GEN-AOT as high as 86.6% in PDLLA matrix and 74.4% in PCL matrix were achieved. While SON resulted in a reduced EE% of GEN-AOT, it was also responsible for a smaller and more homogenous particle size distribution. The use of PDLLA compared with PCL was systematically responsible to an increase of the EE%. This could be attributed to the higher molecular weight of PDLLA, larger size of PDLLA microspheres and physiochemical property differences of the polymers used. The

morphology of all microsphere formulations observed using SEM (Figure 1B) revealed that the surfaces are smooth without presence of pores. As will be explained in further sections of this results section, PCL/GEN-AOT/SON microspheres were chosen for further functionalisation and characterisation. Reproducibility of microsphere fabrication with this methodology was established with further batches showing similar size distributions (0.85 ± 0.46 μm versus 0.80 ± 0.47 μm).

GEN-AOT is diffusing continuously from polyester microspheres

PCL and PDLLA microspheres loaded with GEN-AOT are characterised by a sustained release kinetic (Figure 2A). The GEN-AOT's extremely hydrophobic properties (GEN-AOT solubility in water ≈ 0.43 mg/mL) prevent burst-style releases. Hydrophobic interactions between GEN-AOT and the polymeric matrix are reasoned to result in a more homogenous distribution of the drug in the microspheres. A faster drug release from PCL microspheres is observed compared with PDLLA microspheres. The fabrication method also influenced the drug release kinetics, primarily because of the resulting differences in microsphere size. For example, the PDLLA/GEN-AOT/HSM formulation resulted in the largest microsphere size and EE% (Figure 1), while its release kinetics are the slowest among all tested formulations. The formulation PCL/GEN-AOT/SON had the smallest average microsphere size and underwent the fastest release of antibiotic. This correlates with the hypothesis regarding the enrichment of the drugs at the periphery of the microsphere of crystalline materials like PCL. For a similar weight (i.e. the release experiment was performed on 10 mg), the smallest microspheres have the largest surface area and thus the fastest diffusion-based release of GEN-AOT.

A conventional model used to characterise sustained drug release is the Korsmeyer-Peppas model which is defined by equation (eq. (2))

$$M_t / M_\infty = K_{KP} t^n \tag{2}$$

In which M_t/M_∞ is the cumulative drug released at time t, K_{KP} is the release constant and the n value is used to characterise the type of drug release of the tested system. In Figure 2B, the data of the GEN-AOT release study were logarithmically manipulated (from t^n to $n\log_{10}(t)$ and M_t/M_∞ to $\log_{10}(M_t/M_\infty)$) and averaged, according to the Korsmeyer-Peppas model. When the manipulated data were plotted on a $\log_{10}(M_t/M_\infty)$ versus $\log_{10}(t)$ axis system, linear trendlines with slope n fit the
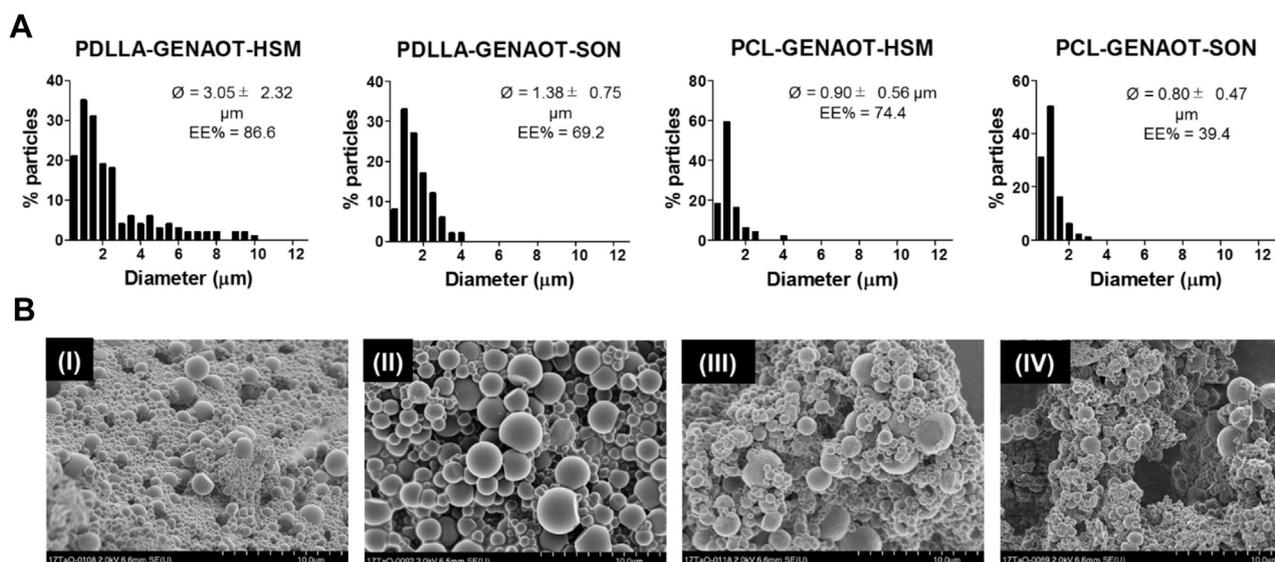

Figure 1. Microsphere size and morphology characterisation. (A) Size distribution histogram (interval = 0.5 μm) of all formulations of microparticles (n = 100). The average microsphere diameter and standard deviation (Ø) and the encapsulation efficiency of the respective antibiotics (EE%) are noted on every histogram. (B) Representative SEM images of PDLLA-GEN-AOT-HSM (I), PDLLA-GEN-AOT-SON (II), PCL-GEN-AOT-HSM (III) and PCL-GEN-AOT-SON (IV). Gen-AOT = gentamicin-dioctyl sulfosuccinate; PCL = poly(ε-caprolactone); SEM = scanning electron microscopy; SON = probe sonication; PDLLA = poly(D,L-lactic acid).
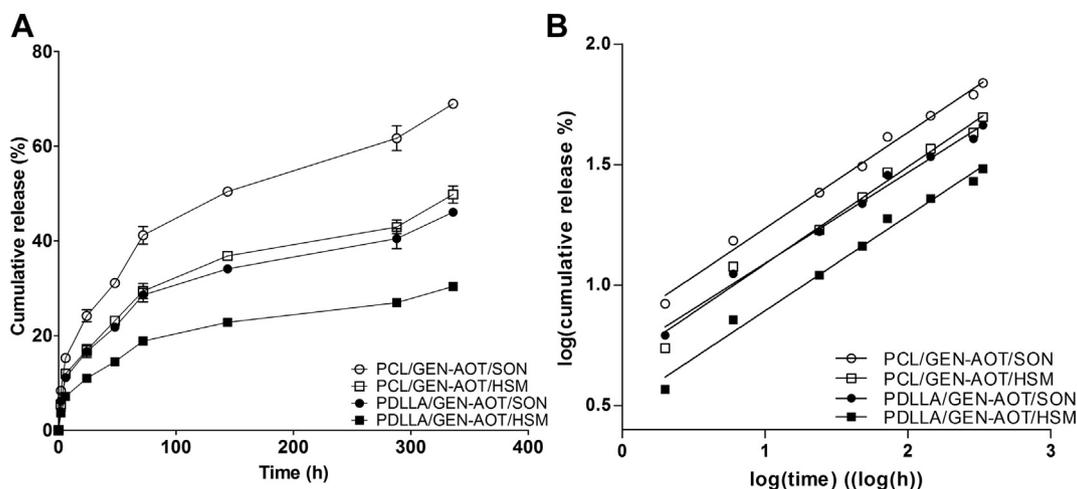
Figure 2. In vitro release profile of GEN-AOT from all microsphere formulations (n = 6). (A) GEN-AOT release profiles from both PCL and PDLLA microspheres. Sustained release of the drug was established after a short burst release in the first 24 h. (B) GEN-AOT release remodelled to fit the Korsmayer-Peppas model for sustained drug release. The trendline fits with high fidelity to the data. Linear trendlines with $R^2 > 0.983$ for all groups was achieved. PDLLA = poly(D,L-lactic acid); Gen-AOT = gentamicin-dioctyl sulfosuccinate; PCL = poly(ε-caprolactone).

experimental data with high precision ($R^2 > 0.983$). Values of n were between 0.31 ± 0.01 (PLA/GEN-AOT/HSM) and 0.40 ± 0.02 (PCL/GEN-AOT/SON), indicating a purely diffusion-based release of drug with negligible effects of polymer erosion (Table 1).

Owing to the higher drug loading capability and the more sustained release of the drug load, PCL microspheres loaded with GEN-AOT and fabricated by probe sonication induced O/W emulsions (SON) were selected for further development into a bone targeting DDS.

Surface functionalisation with ALN optimised for EDC/NHS conjugation

Carboxyl groups on the PCL microsphere surface, necessary for EDC/NHS conjugation, were created by alkaline hydrolysis. The Fourier transform infrared spectroscopy spectrum in Figure 3A shows the shaded peaks that were used to calculate the $C–O/CH_2$ peak area ratios, which are presented Figure 3B. The intensity of CH_2 peaks remains stable after saponification, while a higher presence of OC-O peaks is to be expected. Without exposure to NaOH, the $C–O/CH_2$ ratio is approximately 1.45 ± 0.02, while the ratio increases significantly (unpaired t-test p = 0.017) to 1.61 ± 0.05 after 120 min of 0.1 M NaOH exposure. GPC analysis before and after exposure of PCL microspheres to 0.1 M NaOH revealed that the average polymer degradation of the microspheres was limited. The molecular weight parameters (M_w, M_n and PDI) are listed in Table 2.

Surface morphology of treated microspheres remains smooth without the presence of pores or defects (Figure 3C). To quantify the amount of ALN which can be grafted onto the carboxyl-enriched PCL surface, a fluorescent probe (EDANS) was selected, which exhibits similarities in terms of physiochemical properties and molecular weight (comparison with ALN shown in Figure 3D). Figure 3E shows a schematic of the

reaction that followed the microsphere saponification. The combinational study with varying NaOH treatment durations and EDC/NHS carboxyl activation times (Figure 3F) shows that when both steps are performed for at least 30 min, there is no additional improvement in EDANS functionalisation when prolonging treatment duration. Without saponification, the EDANS fluorescence intensity decreased three-fold, and without EDC/NHS conjugation chemistry, no covalent binding of EDANS occurred.

PCL-ALN microspheres exhibit high HAP binding properties

A scaffold made from porous bone-like material, previously described by our group [23], was used to assess the complexation of PCL-ALN microspheres with HAP (Figure 4A). A 15-fold increase in fluorescence could be measured when PCL-ALN microspheres (loaded with pyrene) were compared with nonfunctionalised microspheres PCL loaded with pyrene after incubation with the scaffold (Figure 4B). The increased fluorescence signals from the bound PCL-ALN microspheres demonstrate that the surface ALN groups are actively involved in chelation to the bone-like material. The presence of microspheres adsorbed onto the surface of the porous HAP scaffold could additionally be observed using SEM (Figure 4C), with chelated PCL-ALN microspheres indicated by the yellow colour. The SEM analysis, together with the increased fluorescence, support the claim that the designed DDS is actively targeting bone mineral.

PCL-ALN microspheres do not hinder bone resorption by osteoclasts

Osteoclast-specific TRAP staining (Figure 5A) showed that in normal osteoclast culture conditions, large and multinucleated cells are formed and are intensely stained. In the presence of 10 μM ALN, the morphology of the osteoclasts became smaller and rounded up, indicating inhibitory and potentially cytotoxic effects of ALN. In the presence of PCL-ALN microspheres, the morphology of osteoclasts remains comparable to untreated cells, which are multinucleated and TRAP positive. A trend was observable for PCL-ALN treated cells to have fewer nuclei or to be smaller in diameter (Figure 5A).

The inhibitory properties of the PCL, PCL-ALN and ALN on the ability of osteoclasts to resorb HAP was showed by a von Kossa staining (example shown in Figure 5B). The data in Figure 5C reveal that the untreated osteoclasts (MCSF) show very high HAP resorption (89.5% of total surface). The presence of 1.7 mg of PCL microspheres reduced the resorptive potential of osteoclasts by approximately 25%. This may be
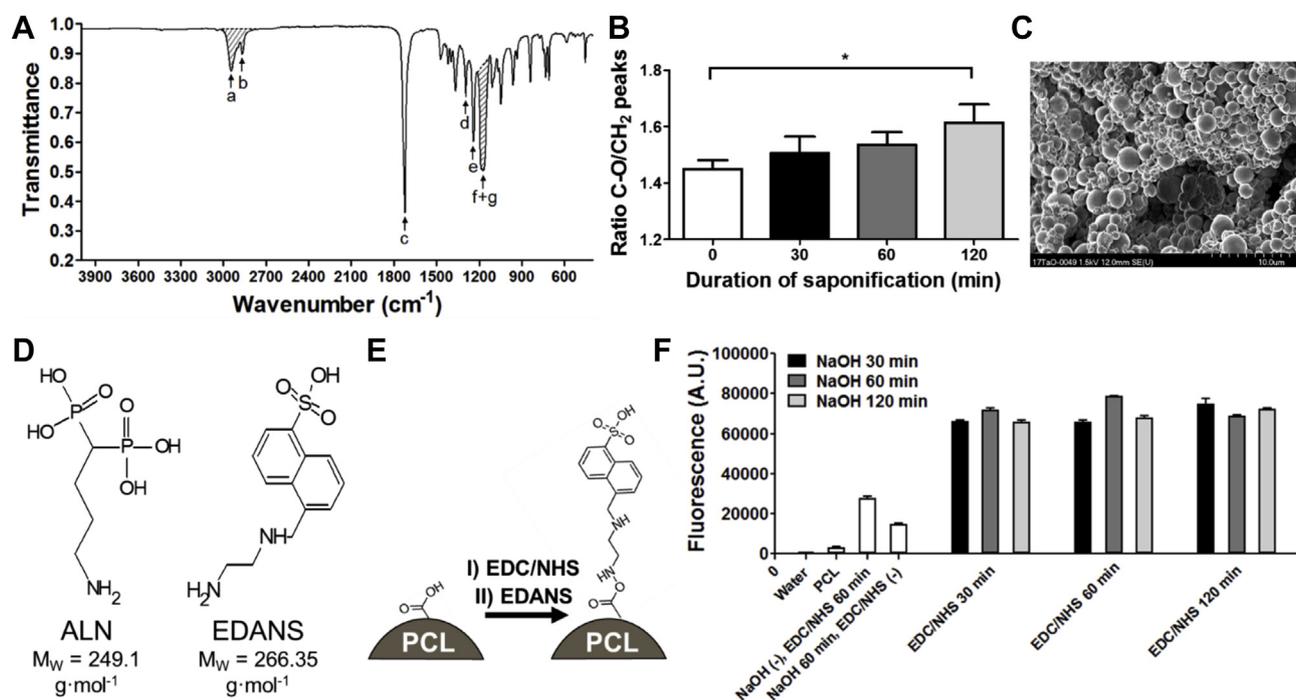
Table 1
Parameters of the release kinetics of Gen-AOT, modelled according to the Korsmeyer-Peppas model. The data are formed from triplicate data whose curves were fitted for each replicate, establishing the reported SD values.

Polymer/Drug/Method	Korsmeyer-Peppas model	
	n	R^2
PCL/Gen-AOT/SON	0.40 ± 0.02	0.988 ± 0.002
PCL/Gen-AOT/HSM	0.33 ± 0.00	0.983 ± 0.005
PLA/Gen-AOT/SON	0.33 ± 0.01	0.987 ± 0.001
PLA/Gen-AOT/HSM	0.31 ± 0.01	0.984 ± 0.003

Gen-AOT = gentamicin-dioctyl sulfosuccinate; SON = probe sonication; HSM = high-speed mechanical mixing by ultra-turrax; PCL = poly(ε-caprolactone).

Figure 3. Surface treatment with NaOH results in an increased presence in carboxylic acid chain ends on the surface of the PCL microspheres, allowing better conjugation with EDANS, a fluorescent model molecule for Alendronate. (A) FTIR spectra of PCL. The labelled peaks represent: a. asymmetric CH_2 stretching, b. symmetric CH_2 stretching, c. carbonyl stretching, d. C–O and C–C stretching in the crystalline phase, e. asymmetric COC stretching, f. OC-O stretching and g. symmetric COC stretching. The combined surface of peaks a and b and the combined surface of peaks f and g were used to calculate the CH_2/C–O ratio which could give an indication to the degree of saponification on the PCL microsphere surface. (B) Semiquantitative analysis of the changes in CH_2 and C–O FTIR peak integral ratio as a result of exposure to 0.1 M NaOH for varying durations (n = 3). (C) PCL microspheres prepared by sonication induced emulsification show no apparent sign of agglomeration or shape-loss after 30 min of exposure to 0.1 M NaOH. NaOH exposure does not result in observable changes to the surface morphology of the microspheres. (D) Molecular structure of ALN and its fluorescent model EDANS. The primary amine on the short carbohydrate tether in both molecules result in similar EDC/NHS based conjugation to the surface of carboxylated PCL microspheres. (E) Conjugation procedure of EDANS to a PCL surface enriched with carboxylic acid groups by NaOH induced saponification. After EDC/NHS activation of surface carboxylic acids, the fluorescent ALN model molecule EDANS was conjugated to the PCL microsphere surface. (F) Fluorescent intensity of the surface conjugated EDANS molecules on PCL microspheres after varying NaOH saponification times and EDC/NHS activation of surface carboxylic acids. FTIR, Fourier transform infrared spectroscopy; PCL = poly(ε-caprolactone); ALN = alendronate; EDC, 1-Ethyl-3-(3-dimethylaminopropyl)carbodiimide; NHS = N-hydroxysuccinimide; EDNAS = (5-((2-Aminoethyl)amino)naphthalene-1-sulfonic acid).

Table 2

Mw, Mn and PDI parameters of PCL microspheres and saponificated PCL microspheres assessed by GPC analysis.

Microsphere group	Mw	Mn	PDI (Mw/Mn)
PCL	84300 g mol^{-1}	47200 g mol^{-1}	1.78
Saponificated PCL	82300 g mol^{-1}	45000 g mol^{-1}	1.83

PCL = poly(ε-caprolactone); GPC = gel permeation chromatography; Mw = weight average molecular weight; Mn = number average molecular weight; PDI = polydispersity index.

because of the precursor cells not forming osteoclasts after phagocytising the PCL microspheres and affecting their differentiation. When the PCL microspheres were functionalised with ALN, the HAP resorption did not differ significantly from the nonfunctionalised group. In contrast, 10 μM ALN further reduced the HAP resorption by approximately 35%. Interestingly, ALN functionalisation of the microspheres did not inhibit resorption greater than PCL alone.

GEN-AOT–loaded PCL microspheres exhibit prolonged antimicrobial properties

The MIC and MIB concentrations of GEN-AOT, its parent drug GEN and the GEN-AOT–loaded PCL microspheres can be found in Table 3.

The evolution of the agar plate zone of inhibition conducted on *S. aureus* demonstrated that when administrated as single dose, GEN-AOT in DMSO solution has a limited duration of antimicrobial effect

(Figure 6A). Prolonged antimicrobial effects were observed for the tested reference materials that are currently employed in clinics. PMMA bone cement (Copal®) loaded with a combination of GEN and vancomycin was responsible for an intermediate ZOI on the *S. aureus* infected agar plates but had a consisted bactericidal effect throughout the 7-day experiment. The GEN-loaded collagen fleece (Garamycin®) released its drug content in a singular burst resulting in very large inhibitory zones in only the first 24 h, followed by a rapid decline of ZOI. This observation supports previous publications, describing that the majority of gentamicin was released from collagen sponge materials after 1.5 h [26]. PCL microspheres loaded with GEN-AOT had an antimicrobial effect up to 5 days (Figure 6B).

Discussion

The current systemic antibiotic therapies for prevention or treatment of bone infection have reduced efficacy because of the combination of low availability at the bony site and the antibiotic's short biological half-lives. Those short-comings make utilisation of antibiotic loaded biomaterials a near mandatory step help OM patients to successfully recover [27]. However, drug release mismatch with desired release patterns, along with lack of biodegradable properties are pressing issues characterising the available DDS. Ideally, the DDS needs to release its complete antibiotic load within 2–3 weeks after implantation to eradicate the bone infection and to prevent subinhibitory antibiotic concentrations leaching from the carrier material in the subsequent periods. Prolonged exposure to antibiotic concentrations below the MIC can promote specific
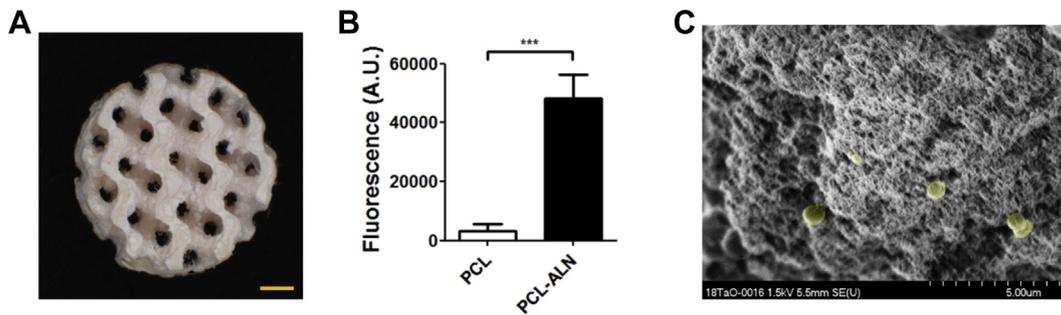
Figure 4. Interaction of ALN functionalised microspheres with HAP-containing substrates. (A) Macroporous methacrylated poly (trimethylene carbonate) scaffold with 40 wt% nano-HAP crystals. The gyroid pore structures, established by stereolithography, could be interpreted as a mimicking structure for trabecular bone. The scalebar represents a length of 1 mm. Pictures republished with permission of [Guillaume et al.]. (B) PCL-ALN microspheres loaded with fluorescent pyrene bound 15 times more effectively to PTMC/40%HAP scaffolds compared to PCL microspheres (unpaired t-test, $\alpha = 0.05$ p = 0.0008). (C) SEM depicting PCL-ALN microspheres bound to a HAP containing substrate. Microparticles were highlighted by artificial yellow colouring using Photoshop CS5. ALN = alendronate; PCL = poly(ε-caprolactone); HAP = hydroxyapatite; SEM = scanning electron microscopy.

antibiotic resistances [28]. The presented DDS aims to overcome these challenges by enhancing drug diffusion kinetics through the utilisation of microsized particles exhibiting large surface area and composed of biodegradable polymers.

In this study, we showed that by varying the nature of the polymer matrix and the emulsion method, we can tailor hydrophobic GEN-AOT release from the fabricated polyester microspheres. PDLLA and PCL materials released the loaded drugs with different release rates. It is hypothesised that drug content in PCL microspheres is more located at the surface of the particle because of its higher crystallinity and is released faster in a diffusion-driven release mechanism. In contrast, once encapsulated in more amorphous PDLLA microspheres, GEN-AOT is better retained in the matrix, resulting in a lower cumulative release in 14 days. This effect, already reported by other groups [29,30], can be explained by differences in microsphere size, polymer crystallinity [31] and molecular weight [32] of the polymers used. It is considered that polymeric matrices with high crystallinity can lead to an increased release of the encapsulated drugs because of the polymer's conformation on the atomic level that expedite the outward diffusion of the drugs [33]. Generally, crystalline materials have poorer drug encapsulation than their amorphous counterparts [29,34], which is supported by the data in Figure 1.
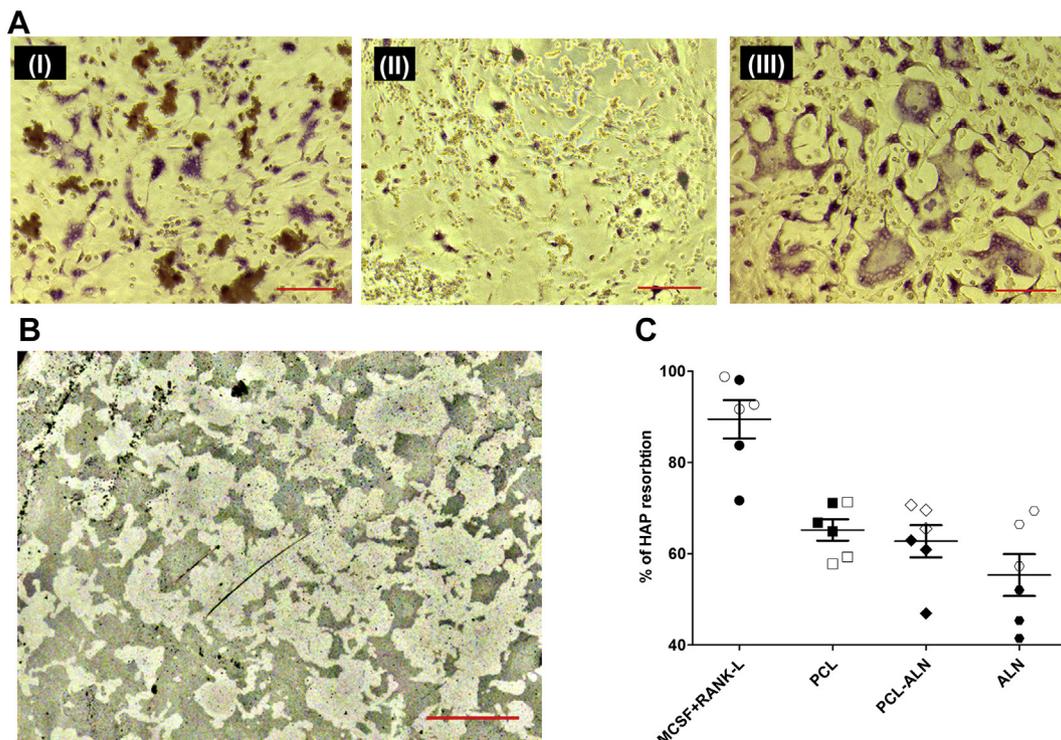

Figure 5. Influence of ALN functionalised PCL microspheres on osteoclastic HAP resorption. (A) Morphology of murine osteoclasts cultured in presence of 1.7 mg PCL-ALN microspheres (I), a 10 μM ALN solution (II) and a control culture without the presence of solubilised ALN or PCL-ALN microspheres (III). Scalebar equals 50 μm. (B) Representative image of a Von Kossa stained Osteoassay® well plate substrate exposed to 1.7 mg PCL-ALN microspheres. The osteoclasts grew for 72 h on the mineral substrate before they were removed. The dark areas are stained remnants of the HAP substrate while the lighter areas show the resorption by the osteoclasts. Scalebar equals 200 μm. (C) Percentage of HAP substrate surface resorbed by osteoclasts in the presence of PCL microparticles, PCL-ALN microparticles or 10 μM ALN solution. MCSF + RANKL group represents a control group without any microparticles or ALN addition. The full and empty symbols represent two murine macrophage donors. ALN = alendronate; RANKL = receptor activator of nuclear factor kappa-B ligand; MCSF, macrophage-colony stimulating factor; PCL = poly(ε-caprolactone); HAP = hydroxyapatite.

Table 3
Susceptibility of *S. aureus* for GEN, GEN-AOT and PCL/GEN-AOT microspheres.

	MIC (µg/mL)	MBC (µg/mL)
GEN	1.95	3.91
GEN-AOT	0.98	0.98
PCL/GEN-AOT microspheres	9.76	19.53

Gen-AOT, gentamicin-dioctyl sulfosuccinate; PCL = poly(ε-caprolactone).

Drug delivery of other hydrophobic drugs like doxorubicin has been investigated, and the relation between DDS parameters and drug release have been reported. Amjadi et al. prepared doxorubicin-loaded PLGA particles in which the lactide content of 50% and 75% was used [32]. Increasing lactide content of the PLGA resulted in lower doxorubicin EE% and lower polydispersity while crystallinity was increased. The release profile of the doxorubicin was faster for the more crystalline PLGA with 75% lactide content compared with the more amorphous PLGA with 50% lactide content. Similar finding was presented by Guillaume et al. [29] comparing the release kinetic and remaining drug retention of another antibiotic (ofloxacin) from amorphous PDLLA versus crystalline PCL, corroborating our results presented here.

The size distribution of the microspheres affects the drug release profile as well. For example, PDLLA-GENAOT-HSM batches with the highest polydispersity and skewed microsphere size distribution showed the slowest release of GEN-AOT. Spiridonova et al. performed extensive modelling on the drug release properties of PLGA delivery vesicles with many geometries, including spherical structures [35]. Findings included that polydisperse spherical systems released their drug slower compared with a more monodisperse system with the same average microsphere diameter. It was reasoned that out-ward diffusion of drug encapsulated in larger microspheres is limited to drug at the periphery of the polymer matrix. This is presumably the reason for the large portion of GEN-AOT that remains unreleased in PDLLA-GENAOT-HSM microspheres. Spiridonova et al. also stated that polydisperse microspheres did significantly not affect drug diffusion in the first hours of release [35], which matches the results presented in this work.

The sustained release of GEN-AOT form both PCL and PDLLA matrices fitted to the Korsmeyer-Peppas model for sustained drug release from polymeric matrices. For spherical systems, values of $n < 0.43$ represent drug release via Fickian diffusion. All four n values of the release profiles are below 0.43, suggesting a release fitting the Fickian diffusion. Low n values could be expected because of the high molecular weight of the PCL and PDLLA polymers and the slow *in vitro* degradation of these polyesters. Ribeiro et al. implemented the Korsmeyer-Peppas model to fit their curcumin release from polyester nanoparticles [36]. With reported n values between 0.31 and 0.40 for different PLGA and PCL compositions, their results are comparable to the data presented in this work.

Average molecular weight of the polymers was only minimally affected by exposure to NaOH, suggesting that saponification was primarily occurring at the microspheres surface. This is in accordance with previous reports on saponification of PCL fibers [37]. EDC/NHS conjugation of ALN to polyester surfaces was optimised in this study. Even though the chemistry is known for decades as an effective conjugation method, protocols vary depending on the nature of the conjugated molecule. While often applied for conjugation of solubilised components, functionalisation of surfaces is less frequently reported. We observed that an increase in saponification time yielded a (slightly) higher carboxylic acid presence on the polyester surface, but it did not influence the binding efficacy of EDANS (fluorophore model for ALN). This observation could be caused by the saturation of the microsphere surface with EDANS because of repulsive forces of the sulfonic acid groups and their negatively charged sulfonate conjugated base. For the targeted application requiring the utilisation of the bone seeker ALN, grafting large amounts of ALN onto the microsphere surface is not essential for an efficient functionality. On the contrary, spherical drug carriers with lower amounts of surface BP groups were shown to be more stable in biological environments and to perform similarly in regard to bone binding efficacy as their counterparts with a denser presence of active surface moieties [38].

The bone binding capacity of the microspheres give potential for targeted drug delivery to bone. However, possible side-effects of ALN on bone homeostasis should be investigated. All BPs are known to inhibit osteoclast ability to resorb bone, which makes them excellent drugs for treating osteoporosis or Paget's disease [39]. Because physiological bone homeostasis is essential during the healing process of OM, it should not be impeded. Hence, using BPs as targeting ligands on DDS needs to be
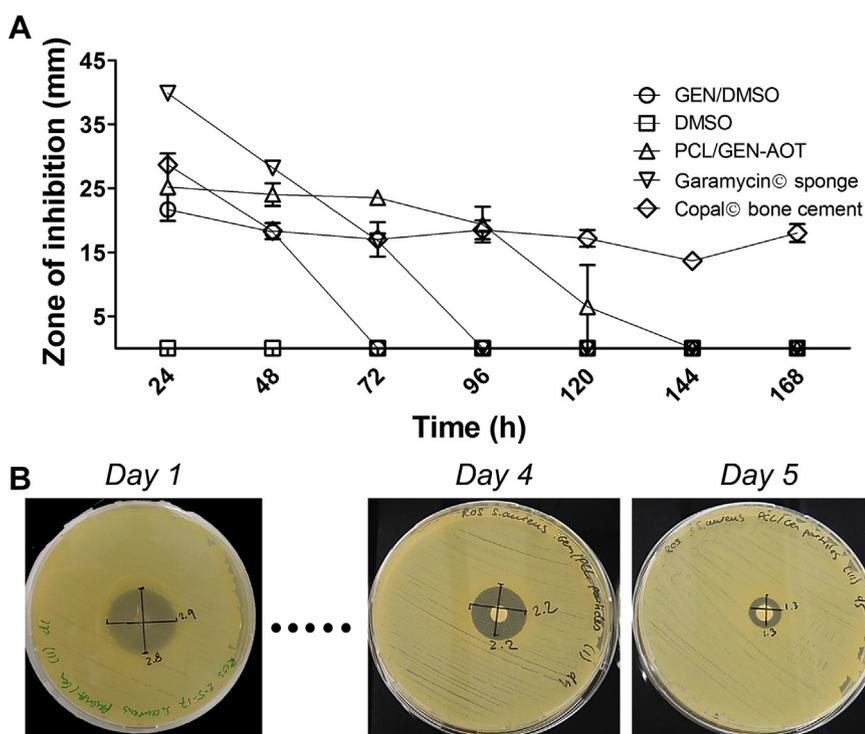

Figure 6. Antimicrobial effect of GEN-AOT–loaded microparticles on Gram positive *S. aureus*. (A) Comparison of the GEN-AOT loaded PCL microspheres to a GEN-AOT solution. The solvent, DMSO, had no measurable inhibitive effect on *S. aureus* colonisation. Garamycin® sponge and Copal Bone cement are two established antibiotic delivery materials. (B) Photographs of the zone of inhibition of *S. aureus* colonisation due to the release of GEN-AOT from PCL microspheres. Wafer containing 1 mg of PCL microspheres loaded with GEN-AOT was transferred daily to an agar plate with freshly plated *S. aureus*. Gen-AOT = gentamicin-dioctyl sulfosuccinate; PCL = poly(ε-caprolactone); DMSO = dimethyl sulfoxide.

cautiously considered. This study describes the effect of PCL-ALN microspheres and ALN solutions on osteoclast formation and their ability to resorb HAP. We show that the presence of a high concentration of PCL microspheres already influences the ability of osteoclasts to resorb bone in a 2D *in vitro* model. After surface functionalisation with ALN, no significant differences were observed in comparison with the PCL group. These results were coherent with findings from Cenni et al., who assessed ALN-functionalised PLGA microspheres [40].

Osteoclasts inherently have broad size distributions, with larger cells being more efficient in bone resorption. When osteoclast size was assessed using TRAP staining, it was observed that the presence of ALN resulted in smaller osteoclasts. Though still observable, this effect was less evident for osteoclasts cultured with PCL-ALN microspheres. These results confirm that when ALN is present on the surface of a polymer construct, it has less detrimental effects on osteoclast growth than when ALN is in solution. This finding can be explained by the fact that the primary amine group of ALN is known to be a promotor of osteoclast inhibition [41,42]. Because the primary amine of ALN is required for the conjugation chemistry to the PCL microspheres, its effect on inhibition of HAP resorption is diminished. Another reason for the similar effects of PCL and PCL-ALN might be the limited amount of ALN that is in direct contact with the HAP substrate and the underlying osteoclasts. A large portion of ALN grafted onto the particle surface is not in direct contact with the osteoclasts on the HAP substrate, hereby potentially reducing the amount of ALN acting on the osteoclasts.

Owing to the sustained release of antibiotic, the MIC and MBC of the developed PCL microspheres with GEN-AOT load is approximately 10 times higher than the MIC and MBC for solubilised GEN-AOT. Interestingly, GEN-AOT showed a lower MIC and MBC as its parent drug GEN. This phenomenon was also observed by Ter Boo et al. and was accredited to the destabilising properties of the AOT ion on the bacterial membrane [9].

Different bacterial strains have been identified to reside at the sites of OM, with the major bacterial strain being *S. aureus* [42]. In terms of antimicrobial activity against *S. aureus*, the PCL microspheres loaded with GEN-AOT was as efficient as the clinical reference materials, e.g. Garamycin® collagen sponge and Copal® bone cement. The microspheres inhibited *S. aureus* for a longer duration than the collagen sponge and had the biodegradable properties that the PMMA bone cement is lacking. Although Copal® bone cement had a longer antimicrobial effect compared with the designed microspheres, GEN-AOT loaded PCL microspheres had a larger zone of inhibition for the initial 4 days of the experiment. The great advantage of the developed PCL microspheres does not only lie in its specific affinity towards bone tissue but also in the fact that its biodegradable properties will make future retrieval surgeries unnecessary, which is beneficial to the patient's recovery process.

Further developments in targeted antibiotic delivery to bone are crucial because of the currently inadequate success rate of OM treatment. This work describes the successful development of antibiotic-loaded PCL and PDLLA microspheres. Sustained *in vitro* antibiotic release allowed for an antimicrobial efficacy against the major OM microbial, *S. aureus,* for up to 5 days. Saponification of the microspheres' surface allowed efficient covalent conjugation of ALN which resulted in 15 times increase in microsphere binding to bone mimicking materials. This shows that our designed DDS can actively bind to HAP and deliver antibiotics to bone mimicking sites. Owing to the versatile nature of the polyester microspheres, other hydrophobic drugs can potentially be encapsulated to optimise the treatment of other bone-related diseases such as osteoporosis or even osteosarcoma.

Conflict of interest statement

The authors have no conflicts of interest to disclose in relation to this article.

Author contribution

S.G.R, D.E and O.G designed the experimental plan. K.T. gave support and guidance to S.G.R regarding all cell culture experiments. Data interpretation and evaluation was done by S.G.R, K.T., T.F.M., D.E and O.G. Both S.G.R and O.G. committed to writing the manuscript. D.W.G and R.G.R. contributed to giving guidance to the research after preliminary data collection. All authors supplied valuable feedback that shaped and gave content to the research and the writing of the final version of the manuscript.

Appendix A. Supplementary data

Supplementary data to this article can be found online at https://doi.org/10.1016/j.jot.2019.07.006.

References

[1] Patzakis M, Zalavras C G. Chronic posttraumatic osteomyelitis and infected nonunion of the tibia: current management concepts, vol. 13; 2005.

[2] Darley ESR, MacGowan AP. Antibiotic treatment of Gram-positive bone and joint infections. J Antimicrob Chemother 2004;53(6):928–35.

[3] Isefuku S, Joyner CJ, Simpson AHRW. Gentamicin may have an adverse effect on osteogenesis. J Orthop Trauma 2003;17(3):212–6.

[4] Hatzenbuehler J, Pulling TJ. Diagnosis and management of osteomyelitis. Am Fam Physician 2011;84(9):1027–33.

[5] Schmidmaier G, Gahukamble AD, Moriarty TF, Richards RG. Infection in fracture fixation: device design and antibiotic coatings reduce infection rates. In: Moriarty TF, Zaat SAJ, Busscher HJ, editors. Biomaterials associated infection: immunological aspects and antimicrobial strategies. New York, NY: Springer New York; 2013. p. 435–53.

[6] Geurts JAP, Walenkamp GHIM. 10 – PMMA beads and spacers for local antibiotic administration. In: Management of periprosthetic joint infections (PJIs). Woodhead Publishing; 2017. p. 219–30.

[7] Ze Liu H, Qi M, Guo B, Hua Liu H. Effects of hydrophilicity/hydrophobicity of a drug on its release from PLGA films 2011;675-677.

[8] Schnieders J, Gbureck U, Thull R, Kissel T. Controlled release of gentamicin from calcium phosphate—poly(lactic acid-co-glycolic acid) composite bone cement. Biomaterials 2006;27(23):4239–49.

[9] Boo G-J, W Grijpma D, Richards R, Moriarty T, Eglin D. Preparation of gentamicin dioctyl sulfosuccinate loaded poly(trimethylene carbonate) matrices intended for the treatment of orthopaedic infections 2015;60.

[10] Imbuluzqueta E, Elizondo E, Gamazo C, Moreno-Calvo E, Veciana J, Ventosa N, et al. Novel bioactive hydrophobic gentamicin carriers for the treatment of intracellular bacterial infections. Acta Biomater 2011;7(4):1599–608 [eng].

[11] Sánchez E, Baro M, Soriano I, Perera A, Évora C. In vivo–in vitro study of biodegradable and osteointegrable gentamicin bone implants. Eur J Pharm Biopharm 2001;52(2):151–8.

[12] Ungaro F, d'Angelo I, Coletta C, d'Emmanuele di Villa Bianca R, Sorrentino R, Perfetto B, et al. Dry powders based on PLGA nanoparticles for pulmonary delivery of antibiotics: modulation of encapsulation efficiency, release rate and lung deposition pattern by hydrophilic polymers. J Control Release 2012;157(1): 149–59.

[13] Chang HI, Perrie Y, Coombes AGA. Delivery of the antibiotic gentamicin sulphate from precipitation cast matrices of polycaprolactone. J Control Release 2006; 110(2):414–21.

[14] Cha Y, Pitt CG. The biodegradability of polyester blends. Biomaterials 1990;11(2): 108–12.

[15] Rotman SG, Grijpma DW, Richards RG, Moriarty TF, Eglin D, Guillaume O. Drug delivery systems functionalized with bone mineral seeking agents for bone targeted therapeutics. J Control Release 2018;269:88–99.

[16] Yewle JN. Bifunctional bisphosphonates for delivering biomolecules to bone. PhD thesis. Lexington: College of Arts and Sciences at the University of Kentucky; 2012.

[17] Choi SW, Kim JH. Design of surface-modified poly(D,L-lactide-co-glycolide) nanoparticles for targeted drug delivery to bone. J Control Release 2007;122(1):24–30.

[18] de Miguel L, Noiray M, Surpateanu G, Iorga BI, Ponchel G. Poly(γ-benzyl-l-glutamate)-PEG-alendronate multivalent nanoparticles for bone targeting. Int J Pharm 2014;460(1–2):73–82.

[19] Thamake SI, Raut SL, Gryczynski Z, Ranjan AP, Vishwanatha JK. Alendronate coated poly-lactic-co-glycolic acid (PLGA) nanoparticles for active targeting of metastatic breast cancer. Biomaterials 2012;33(29):7164–73.

[20] Pranatharthiharan S, Patel MD, Malshe VC, Pujari V, Gorakshakar A, Madkaikar M, et al. Asialoglycoprotein receptor targeted delivery of doxorubicin nanoparticles for hepatocellular carcinoma. Drug Deliv 2017;24(1):20–9 [eng].

[21] Moshiri A, Sharifi AM, Oryan A. Role of Simvastatin on fracture healing and osteoporosis: a systematic review on in vivo investigations. Clin Exp Pharmacol Physiol 2016;43(7):659–84.

[22] Segal E, Pan H, Benayoun L, Kopečková P, Shaked Y, Kopeček J, et al. Enhanced anti-tumor activity and safety profile of targeted nano-scaled HPMA copolymer-alendronate-TNP-470 conjugate in the treatment of bone malignances 2011;32.

[23] Guillaume O, Geven MA, Sprecher CM, Stadelmann VA, Grijpma DW, Tang TT, et al. Surface-enrichment with hydroxyapatite nanoparticles in stereolithography-fabricated composite polymer scaffolds promotes bone repair. Acta Biomater 2017;54:386–98.

[24] Sampath SS, Robinson DH. Comparison of new and existing spectrophotometric methods for the analysis of tobramycin and other aminoglycosides. J Pharm Sci 1990;79(5):428–31 [eng].

[25] Guillaume O, Geven M, Grijpma DW, Tang T, Qin L, Lai Y-X, et al. Poly(trimethylene carbonate) and nano-hydroxyapatite porous scaffolds manufactured by stereolithography. Polym Adv Technol 2016;28:1219–25.

[26] Sorensen TS, Sorensen AI, Merser S. Rapid release of gentamicin from collagen sponge. In vitro comparison with plastic beads. Acta Orthop Scand 1990;61(4):353–6.

[27] Neut D, Kluin OS, Crielaard BJ, van der Mei HC, Busscher HJ, Grijpma DW. A biodegradable antibiotic delivery system based on poly-(trimethylene carbonate) for the treatment of osteomyelitis. Acta Orthop 2009;80(5):514–9.

[28] Bistolfi A, Massazza G, Vernè E, Massè A, Deledda D, Ferraris S, et al. Antibiotic-loaded cement in orthopedic surgery: a review, vol. 2011; 2011.

[29] Guillaume O, Lavigne JP, Lefranc O, Nottelet B, Coudane J, Garric X. New antibiotic-eluting mesh used for soft tissue reinforcement. Acta Biomater 2011;7(9):3390–7.

[30] Liggins RT, Burt HM. Paclitaxel loaded poly(l-lactic acid) (PLLA) microspheres: II. The effect of processing parameters on microsphere morphology and drug release kinetics. Int J Pharm 2004;281(1):103–6.

[31] Yan J, Ye Z, Chen M, Liu Z, Xiao Y, Zhang Y, et al. Fine tuning micellar core-forming block of poly(ethylene glycol)-block-poly(ε-caprolactone) amphiphilic copolymers based on chemical modification for the solubilization and delivery of doxorubicin. Biomacromolecules 2011;12(7):2562–72.

[32] Sunoqrot S, Alsadi A, Tarawneh O, Hamed R. Polymer type and molecular weight dictate the encapsulation efficiency and release of Quercetin from polymeric micelles. Colloid Polym Sci 2017;295(10):2051–9.

[33] Sinha VR, Bansal K, Kaushik R, Kumria R, Trehan A. Poly-ε-caprolactone microspheres and nanospheres: an overview. Int J Pharm 2004;278(1):1–23.

[34] Korzhikov V, Averianov I, Litvinchuk E, Tennikova TB. Polyester-based microparticles of different hydrophobicity: the patterns of lipophilic drug entrapment and release. J Microencapsul 2016;33(3):199–208.

[35] Spiridonova TI, Tverdokhlebov SI, Anissimov YG. Investigation of the size distribution for diffusion-controlled drug release from drug delivery systems of various geometries. J Pharm Sci 2019;108(8).

[36] Ribeiro CAS, de Castro CE, Albuquerque LJC, Batista CCS, Giacomelli FC. Biodegradable nanoparticles as nanomedicines: are drug-loading content and release mechanism dictated by particle density? Colloid Polym Sci 2017;295(8):1271–80.

[37] Bosworth LA, Hu W, Shi Y, Cartmell SH. Enhancing biocompatibility without compromising material properties: an optimised NaOH treatment for electrospun polycaprolactone fibres. J Nanomater 2019;2019:11.

[38] Yin Q, Tang L, Cai K, Tong R, Sternberg R, Yang X, et al. Pamidronate functionalized nanoconjugates for targeted therapy of focal skeletal malignant osteolysis. Proc Natl Acad Sci 2016;113(32).

[39] Fleisch H. Bisphosphonates in bone disease: from laboatory to the patient. 2nd ed. Carnforth: The Parthenon publishing group Ltd.; 1995.

[40] Cenni E, Avnet S, Granchi D, Fotia C, Salerno M, Micieli D, et al. The effect of poly(d,l-lactide-co-glycolide)-alendronate conjugate nanoparticles on human osteoclast precursors. J Biomater Sci Polym Ed 2012;23(10):1285–300.

[41] Drake MT, Clarke BL, Khosla S. Bisphosphonates: mechanism of action and role in clinical practice. Mayo Clin Proc Mayo Clin 2008;83(9):1032–45.

[42] Dunford JE, Thompson K, Coxon FP, Luckman SP, Hahn FM, Poulter CD, et al. Structure-activity relationships for inhibition of farnesyl diphosphate synthase in vitro and inhibition of bone resorption in vivo by nitrogen-containing bisphosphonates. J Pharmacol Exp Ther 2001;296(2):235–42 [eng].